

Supplementary Material for

***Staphylococcus aureus* induces drug resistance in cancer T cells in
Sézary Syndrome**

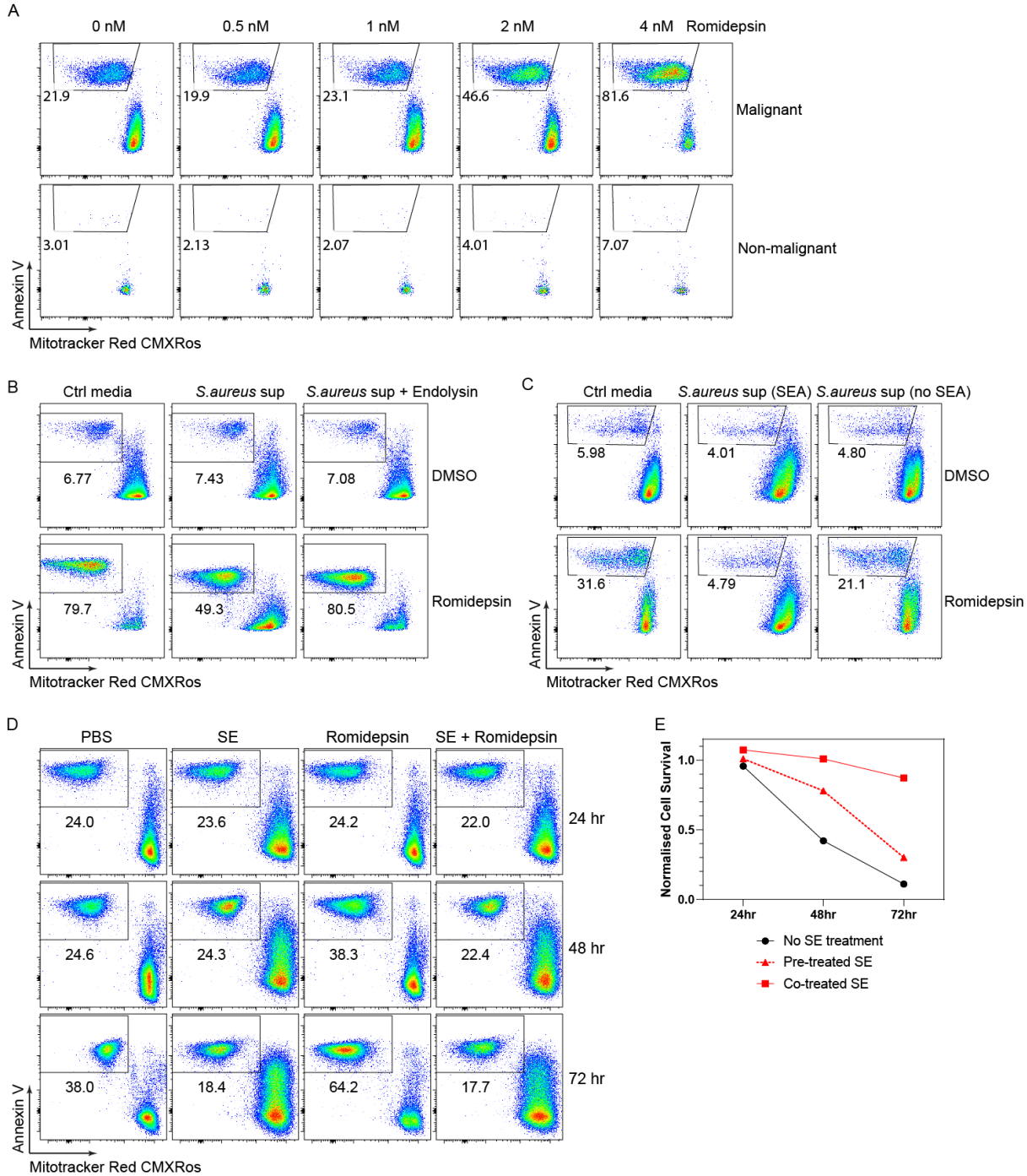
Chella Krishna Vadivel et al.

<https://doi.org/10.1182/blood.2023021671>

Contents

Supplementary Figures and legends	1
Supplementary figure 1: <i>S. aureus</i> culture supernatants and SE induce drug resistance in malignant T cells.....	2
Supplementary figure 2: SE largely overrides the transcriptional effect of romidepsin in malignant T cells.....	3
Supplementary figure 3: SE-induced malignant cells from blood resemble cells in skin.	4
Supplementary figure 4: SE-mediated drug resistance of malignant T cells is not limited to romidepsin.....	6
Supplementary figure 5: SE-induced drug resistance is independent of MEK and TLR 2/4 signaling.	7
Supplementary figure 6: SE-induced drug resistance can be either JAK-dependent or -independent.	8
Supplementary figure 7: SE induces drug resistance in purified malignant T cell cultures via JAK dependent or independent mechanisms.	9
Supplementary Methods	10
PBMC cryopreservation	10
Anti- <i>S. aureus</i> IgG ELISA.....	10
Cytokine analysis.....	11
Proliferation assay.....	11
CITE-seq library preparation and sequencing.	11
CITE-seq pre-processing and filtering.	11
CITE-seq differential gene expression, gene-set enrichment, and transcription factor activity analysis and HDACi resistance gene-set scoring.	12
HDACi resistance gene-sets:.....	13
Supplementary References	13

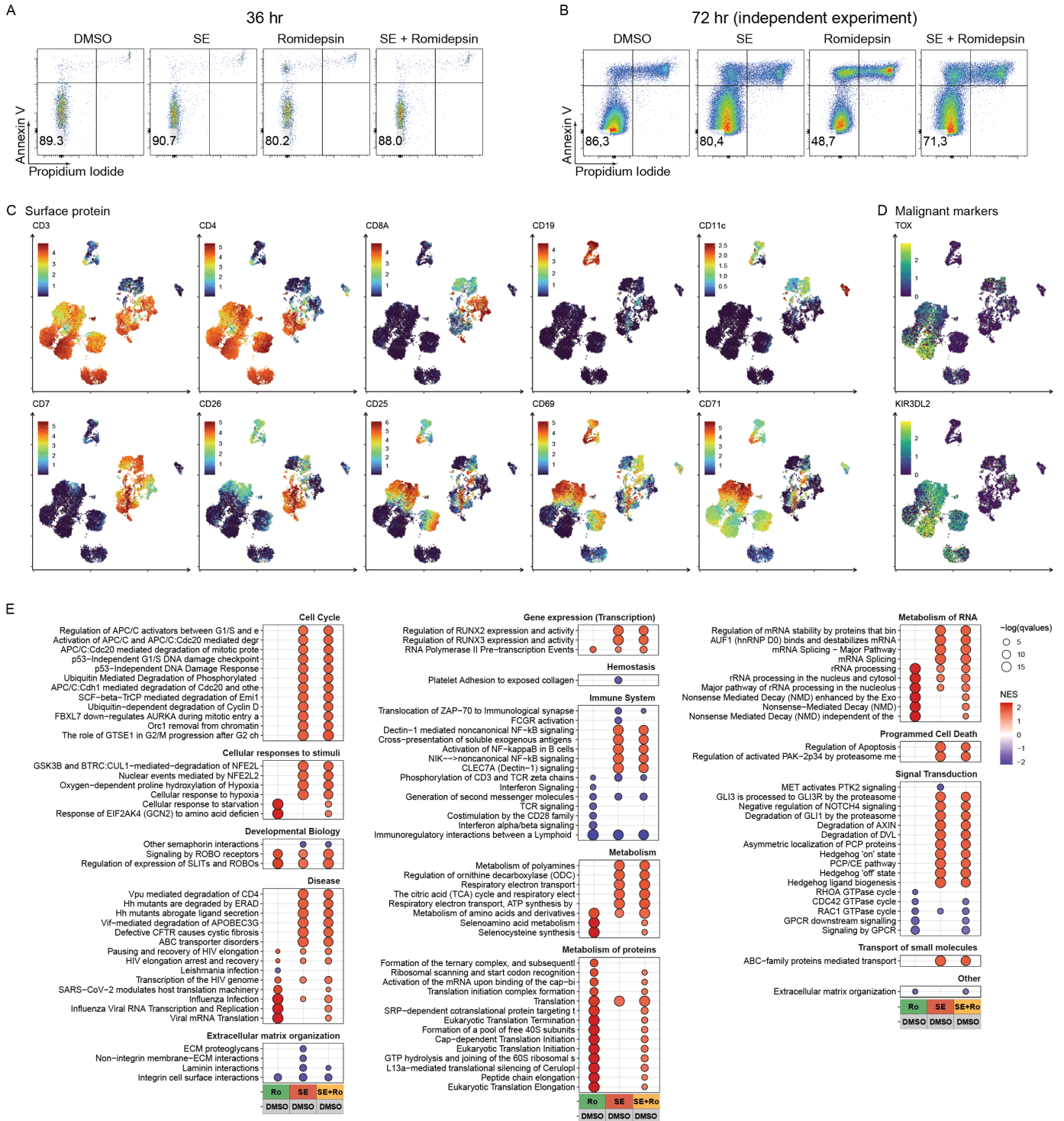
Supplementary figure 1



Supplementary figure 1: *S. aureus* culture supernatants and SE induce drug resistance in malignant T cells.

A. Flow cytometric plots showing apoptotic fraction of malignant and nonmalignant T cells from SS8 PBMCs following 72 hours of treatment with increasing concentrations of romidepsin in the presence (SE) or absence (PBS) of staphylococcal enterotoxins (SE). **B.** Flow cytometric plots showing apoptotic fraction of malignant T cells from SS13 PBMCs following 72 hours of treatment with 2 nM romidepsin and bacterial culture supernatant (sup) from *S. aureus* cultured in the presence or absence of endolysin. The utilized *S. aureus* strain was originally isolated from lesional skin of a different SS patient. **C.** Flow cytometric plots showing apoptotic fraction of malignant T cells from SS8 PBMCs following 72 hours of treatment with 2 nM romidepsin and bacterial culture supernatant from *S. aureus* strains which produce (*S. aureus* sup (SEA)) or did not produce SEA (*S. aureus* sup (no SEA)). **D.** Flow cytometric plots showing apoptotic fraction of malignant T cells from SS12 (left) and SS4 (right) PBMCs following 24, 48 and 72 hours of treatment with 2 nM romidepsin in the presence or absence of SE. **E.** Kinetics showing normalized malignant cell survival following 2 nM romidepsin treatment of SS4 PBMC after 24, 48 and 72 hours with either pre-treated SE (for 72 hours) or added along with Romidepsin (Co-treated SE) or no SE.

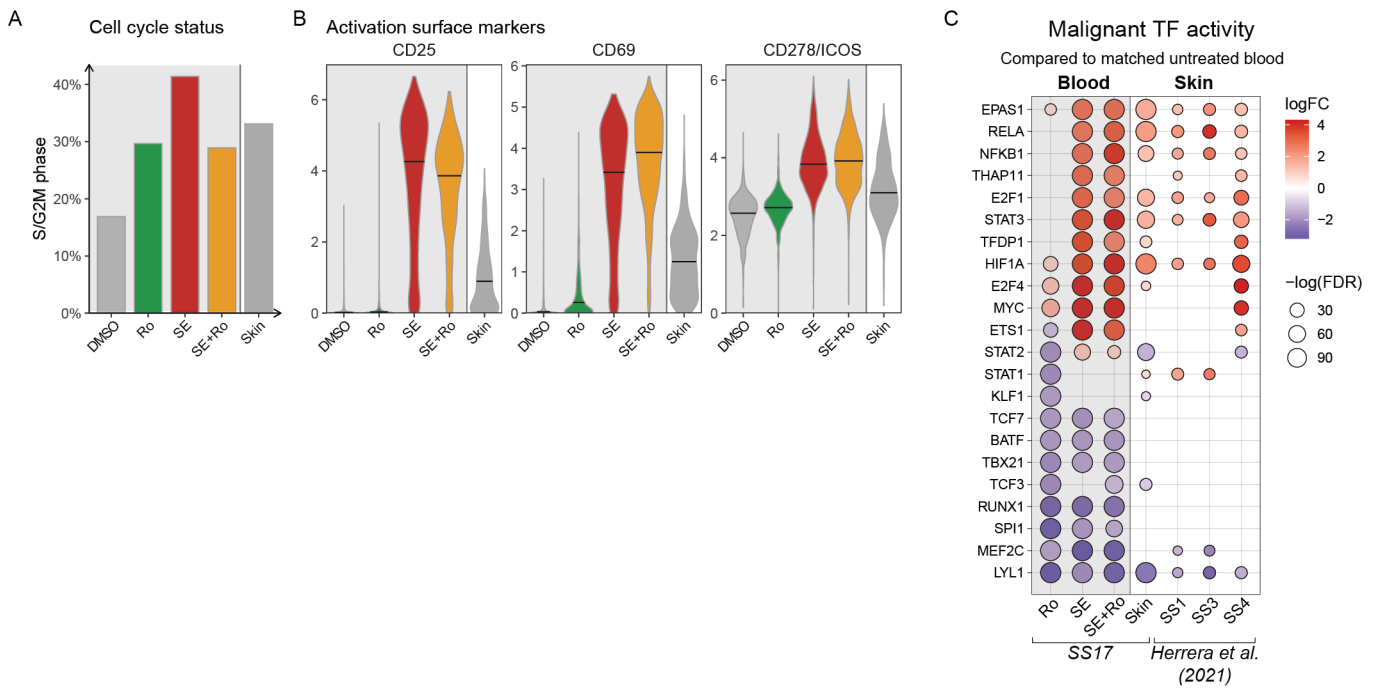
Supplementary figure 2



Supplementary figure 2: SE largely overrides the transcriptional effect of romidepsin in malignant T cells.

A, B. Flow cytometric plots showing SS17 PBMCs treated with 2 nM romidepsin for (A) 36 or (B) 72 hours in the presence or absence of staphylococcal enterotoxins (SE). **B.** Independent experiment from same SS patient PBMCs as used in (A) following cryopreservation. **C, D.** Uniform Manifold Approximation and Projection (UMAP) calculated based on both mRNA and surface protein expression using totalVI colored by (C) TotalVI denoised protein expression of lineage (CD3, CD4, CD8A, CD19 and CD11c), malignant (CD7 and CD26) and T cell activation markers (CD25, CD69 and CD71) as well as (D) normalized mRNA expression of malignant associated genes, TOX and KIR3DL2. **E.** Gene Set Enrichment analysis (GSEA) of Reactome pathways comparing three treatment conditions after 36 hours of culture: romidepsin (Ro), SE and SE+Ro with PBS treated control. Plot shows top 50 pathways from each comparison based on highest absolute normalized enrichment scores (NES) having a q-value below 0.05.

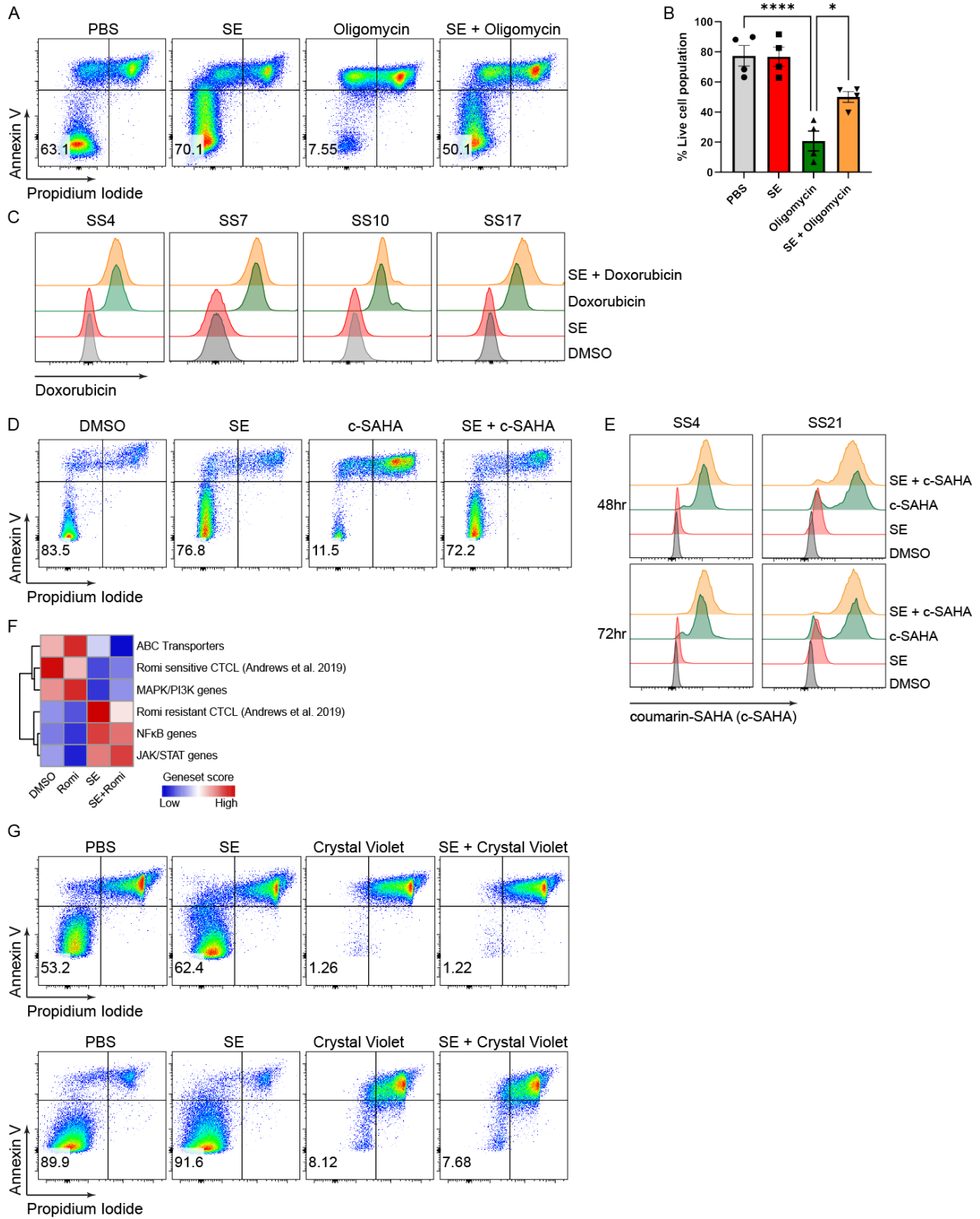
Supplementary figure 3



Supplementary figure 3: SE-induced malignant cells from blood resemble cells in skin.

A. Fraction of malignant cells in active cell cycle (S or G2/M phase) inferred from CITE-seq gene expression and **(B)** expression of activation markers (surface protein expression of CD25, CD69 and CD278/ICOS) from PBMCs treated with Romidepsin in the presence or absence of SE as well as in a matched skin biopsy from SS17. **C.** Transcription factor activity analysis using DoRothEA transcription factor signatures comparing three treatment conditions from SS17 PBMCs after 36 hours of culture: Ro, SE, and SE+Ro with DMSO treated control (also shown in Figure 3H) as well as comparisons between malignant cells from matched skin and blood from SS17 as well as three additional SS patients from a previously published cohort (Herrera et al. 2021, Blood). Plot shows top 10 differentially activated transcription factors from each blood comparison based on highest absolute log2 fold change having an FDR below 0.05. To allow visualization of activities from samples with lower cell numbers (skin samples), extreme FDR values were set to a lower limit of 10-50.

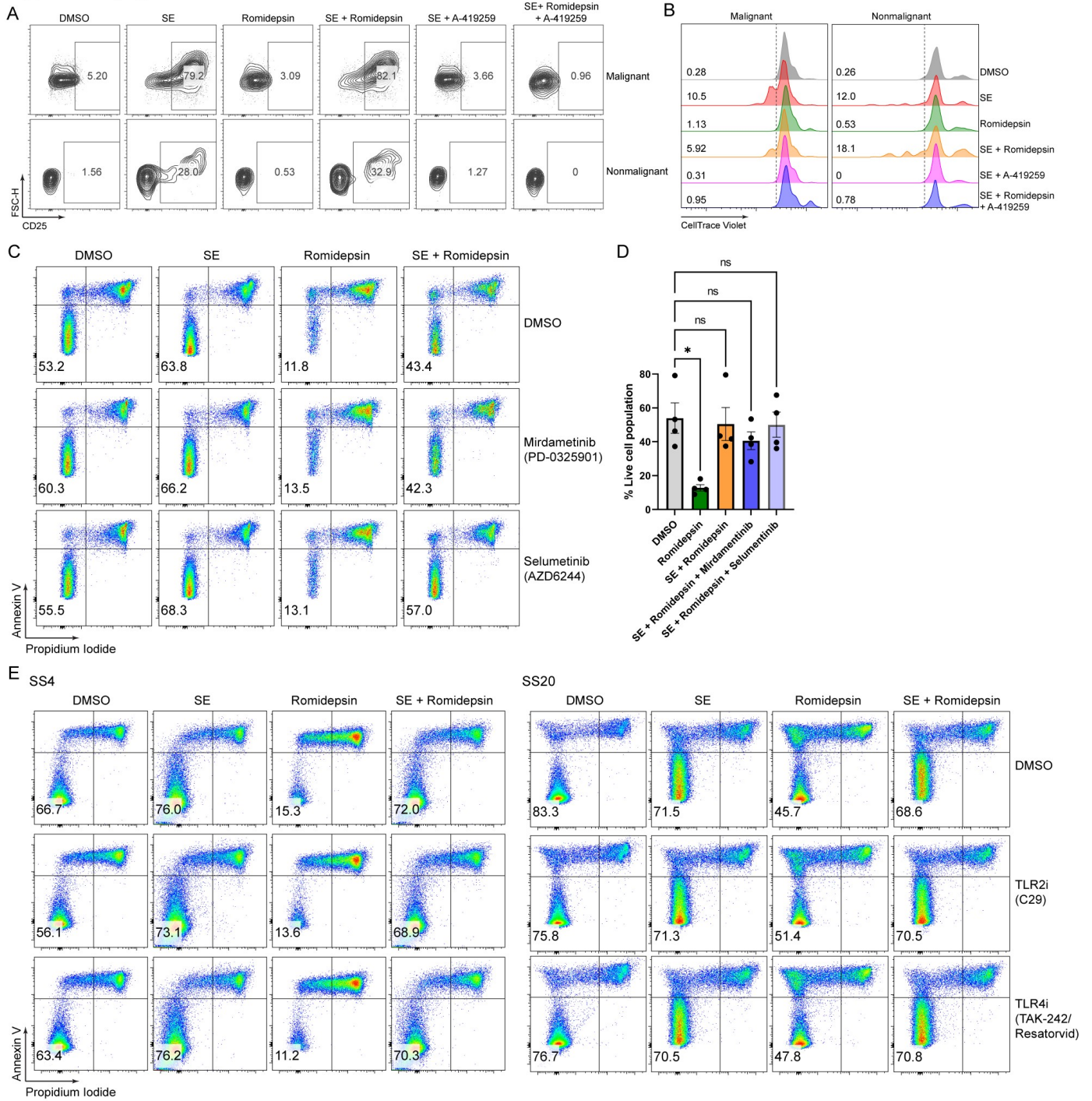
Supplementary figure 4



Supplementary figure 4: SE-mediated drug resistance of malignant T cells is not limited to romidepsin.

A, B. Representative flow cytometric plots (**A**, SS12) and quantifications (**B**) of percentage of viable malignant cells from SS patients PBMCs cultured for 72 hours in the presence or absence of staphylococcal enterotoxins (SE) and treated with 1 μ M oligomycin (n=4 [SS7, SS11, SS12, SS17]). Statistical significance was assessed by ordinary one-way ANOVA followed by Tukey's multiple comparisons test. *P<0.05, ****P<0.0001. **C.** Histograms showing doxorubicin levels in malignant cells from SS patients PBMCs cultured for 72 hours in the presence or absence of staphylococcal enterotoxins (SE) and treated with Doxorubicin. **D.** Flow cytometric plots showing percentage of viable malignant cells from SS4 PBMCs cultured for 72 hours in the presence or absence of staphylococcal enterotoxins (SE) and treated with 1 μ M coumarin-SAHA (c-SAHA). **E.** Histograms showing SAHA levels in malignant cells from SS PBMCs in the presence or absence of staphylococcal enterotoxins (SE) and c-SAHA treatment for 72 hours. **F.** Heatmap of mean HDACi resistance-related gene-set scores within malignant cells from each sample condition (DMSO, Romidepsin (Romi), SE and SE+Romi) included in the SS17 CITE-seq experiment. Color indicates row-scaled mean scores for each gene-set. Genes included in each gene-set are included in supplementary materials and methods and were calculated using the UCell R package. **G.** Flow cytometric plots showing percentage of viable malignant cells from SS10 (top) and SS11(bottom) PBMCs cultured for 72 hours in the presence or absence of staphylococcal enterotoxins (SE) and treated with 1 μ M crystal violet.

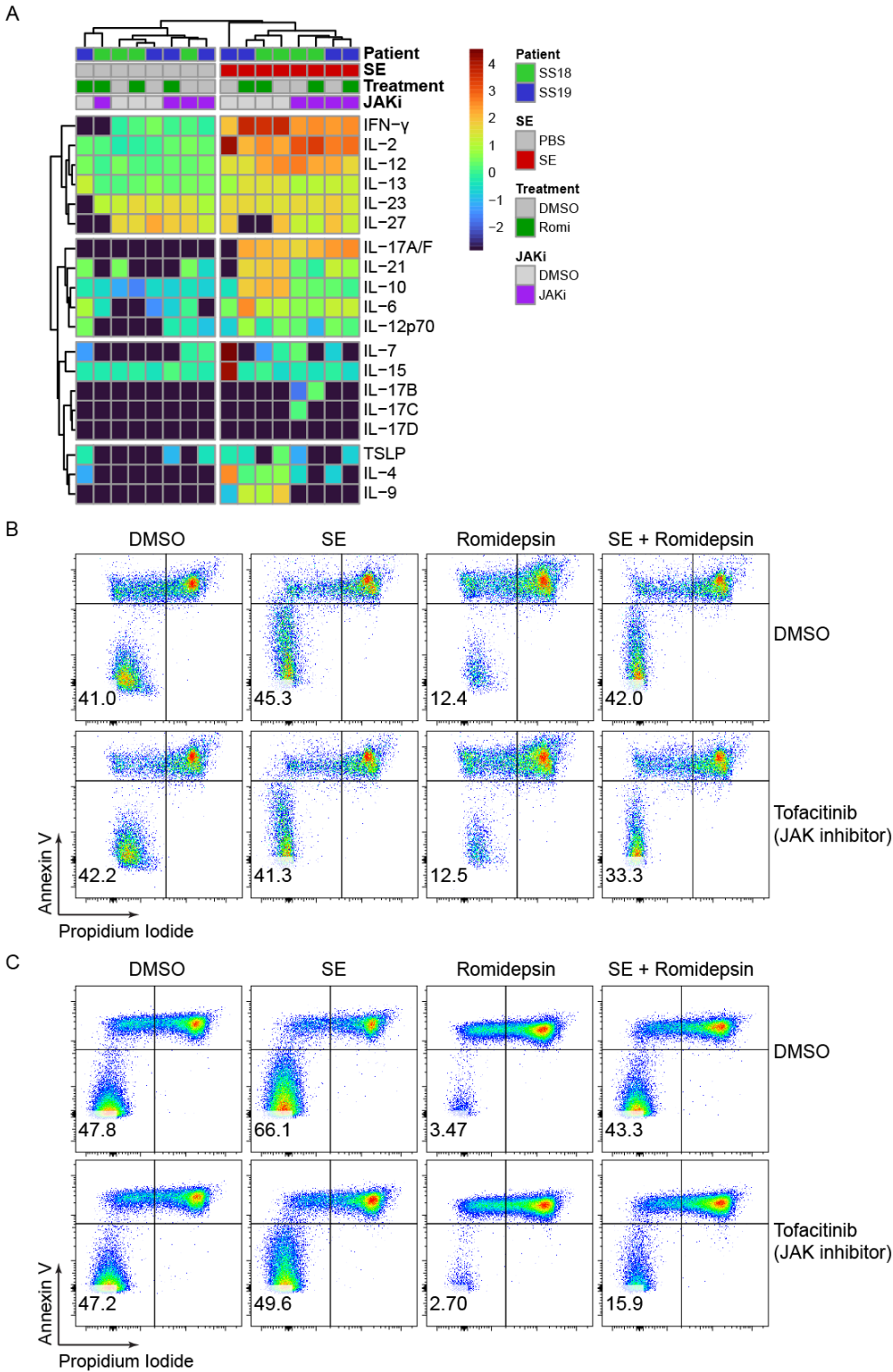
Supplementary figure 5



Supplementary figure 5: SE-induced drug resistance is independent of MEK and TLR 2/4 signaling.

A, B. Flow cytometric plots showing (A) CD25+ and (B) histogram levels of CellTrace Violet (values showing percent of malignant cells undergone cell division) in malignant and nonmalignant CD4+ T cells from SS12 PBMCs treated with 2 nM romidepsin for 72 hours in the presence or absence of staphylococcal enterotoxins (SE) and 2 μM SRC inhibitor (A-419259). **C, D.** Representative flow cytometric plots (C, SS10) and quantifications (D) of percentage of viable malignant cells from four SS patients PBMCs (SS4, SS8, SS10, SS12) treated with 2 nM romidepsin for 72 hours in the presence or absence of staphylococcal enterotoxins (SE) and MEK inhibitors (0.5 μM mirdametinib & 0.5 μM selumetinib). Statistical significance was assessed by Friedman test followed by Dunn's multiple comparisons test. *P<0.05. **E.** Flow cytometric plots showing percentage of viable malignant cells from SS4 (left) and SS20 (right) PBMCs treated with 2 nM romidepsin for 72 hours in the presence or absence of staphylococcal enterotoxins (SE) and treated with either TLR2 inhibitor (10 μM C29) or TLR4 inhibitor (10 μM TAK-242/Resatorvid).

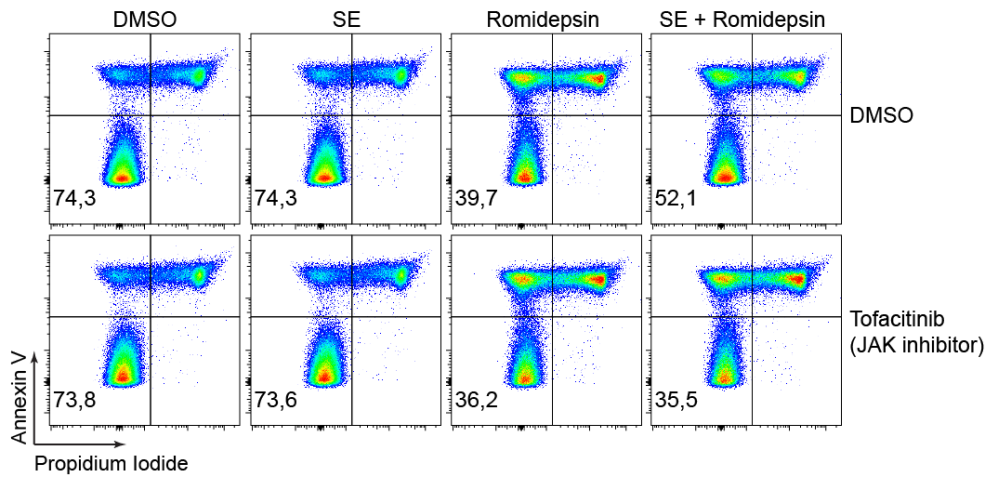
Supplementary figure 6



Supplementary figure 6: SE-induced drug resistance can be either JAK-dependent or -independent.

A. Heatmap showing cytokines secreted by SS PBMCs following 72 hr treatment with 2 nM Romidepsin (Romi) in the presence or absence of Staphylococcal enterotoxins (SE) and treated with and without 1 μ M JAK inhibitor (Tofacitinib, JAKi). **B, C.** Flow cytometric plots showing percentage of viable malignant cells from SS patients PBMCs treated with 2 nM romidepsin for 72 hours in the presence or absence of staphylococcal enterotoxins (SE) and JAK inhibitor (1 μ M tofacitinib) of patients exhibiting (**B**) JAK-independent (SS12) or (**C**) JAK-dependent (SS4) resistance being induced by the presence of SE.

Supplementary figure 7



Supplementary figure 7: SE induces drug resistance in purified malignant T cell cultures via JAK dependent or independent mechanisms.

Flow cytometric plots showing percentage of viable malignant cells from sorted malignant T cells of SS15 treated with 2 nM romidepsin for 72 hours in the presence or absence of staphylococcal enterotoxins (SE) and JAK inhibitor (1 μ M tofacitinib).

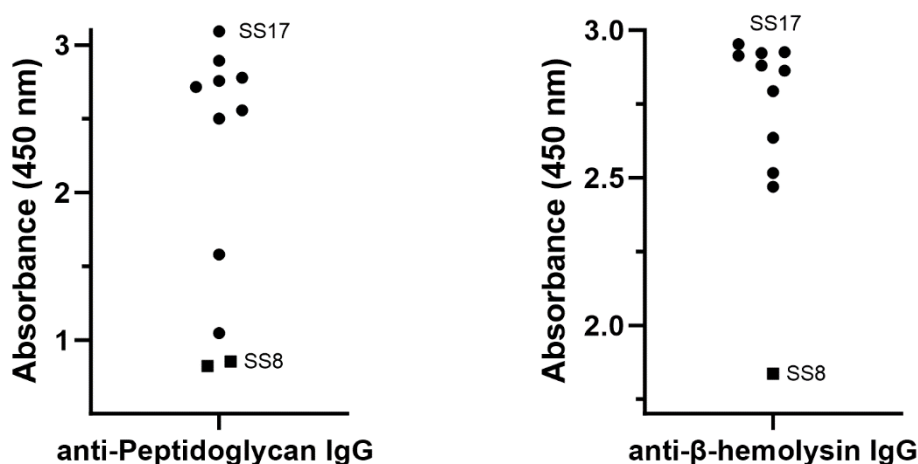
Supplementary Methods

PBMC cryopreservation

In most cases, after isolation, PBMCs were cryopreserved in vials with a preservative media (RPMI media with 30% human serum and 20% dimethyl sulfoxide) and stored in either liquid nitrogen tanks or -150⁰ C freezer. For experiments, cryopreserved PBMC vials were taken out of the freezer, quickly thawed in a 37⁰ C water bath, and washed twice in RPMI media by centrifugation and then resuspended in culture media.

Anti-*S. aureus* IgG ELISA

For assessing IgG levels against *S. aureus* in patients' sera, ELISA was performed with some modifications from a published study¹. Peptidoglycan and β -hemolysin (Toxin Technology) were coated at 2 μ g/mL concentration (100 μ L volume per well) in a 96 well ELISA plates (ThermoFischer) at 4⁰ C overnight. Plates were washed for five times in PBS containing 0.05% Tween-20 and blocked with 2% bovine serum albumin (300 μ L) for an hour at room temperature in a plate shaker at 50 rpm. Sera from patients (100 μ L) were then added along with controls (Bacteremia SS patient serum, human IgG isotype (BioLegend), human umbilical cord serum (Anogen Yes Biotech Laboratories)) to the coated wells and the plate was incubated for 1.5 hours at room temperature in a plate shaker at 50 rpm. Plates were then washed 5 times and then incubated with goat anti-human IgG Fc HRP antibody (Sigma Aldrich) at 1:5000 dilution at a volume of 100 μ L for 1 hour in a plate shaker at 50 rpm. After incubation, plates were washed 5 times and 100 μ L TMB HRP substrate (Kementec) was added. Color development was followed for 10 to 15 minutes and then 50 μ L stop solution (1M H₂SO₄) was added. Absorbance was measured at 450 nm with an ELISA microplate reader (BMG Labtech).



Supplementary methods figure 1: Plots showing ELISA absorbance values for IgG antibody against *S. aureus* peptidoglycan and β -hemolysin in SS patient sera.

Cytokine analysis

Cell culture supernatants were collected at the end of experiments and were stored in -80°C . Mesoscale human V-plex assay kits (Meso Scale Discovery) were used to analyse cytokines in stored cell culture supernatants according to manufacturer's protocol.

Proliferation assay

For cell proliferation, CellTrace Violet (ThermoFisher Scientific) was used following manufacturer's protocol. Briefly, SS PBMCs were stained with CellTrace Violet for 10 minutes in a serum free RPMI media at 37°C . The remaining CellTrace Violet is quenched by adding human serum and incubation for 5 minutes. Cells were washed and experimental procedure was carried out.

CITE-seq library preparation and sequencing.

The five conditions were hashtagged with unique oligo-conjugated antibodies targeting ubiquitously expressed surface protein ($\beta 2$ Microglobulin; see table below) to allow multiplexing of all samples into the same cell segmentation using the 10X Chromium platform as previously described². Equal numbers of viable cells (Annexin V- & Propidium Iodide-negative) from each condition were FACS sorted into 96 well plate together with other multiplexed samples. Volume was reduced by centrifugation and pooled samples were loaded into two reaction wells on a 10X Chromium Chip K following manufacturer's instructions. After cDNA synthesis, emulsion recovery and clean up, full length cDNA was amplified by 13 cycles of PCR with addition of 25 nM of primers targeting the PCR handle present on all the hashtag oligo (HTO) antibodies (HTO_add: GTGACTGGAGTTCAGACGTGTGCTCTAATGTTGGG*A*C) and antibody-derived tags (ADT; TotalSeq-C) antibodies (ADT_add: CTCGTGGGCTCGGAGATGTGTATAAGAG*A*C) together with the cDNA primers included in the Chromium Next GEM Single Cell 5' reagent kit v2 (10X Genomics). Following size-selection, HTO and ADT sequencing libraries were constructed separately from the small cDNA fraction by 9 and 12 cycles of PCR using TruSeq/TruSeq and TruSeq/Nextera P5/P7 indexing primers, respectively. Gene expression (GEX) and TCR $\alpha\beta$ sequencing libraries were constructed from the large cDNA fraction following manufacturer's instructions. HTO, ADT, GEX and TCR $\alpha\beta$ from both reactions were sequencing together on an Illumina NovaSeq6000 SP flow cell at a mixing ratio of 10:10:40:1.

<i>Sample</i>	Hashtag	Barcode
<i>PBS_36h</i>	HTO-01	CATTGTATGCAG
<i>SE_36h</i>	HTO-02	TCTATTGAGCTT
<i>Romidepsin_36h</i>	HTO-03	ACGATTCATCAG
<i>Romidepsin+SE_36h</i>	HTO-04	TGGTTGAAGCTG
<i>Skin_36h</i>	HTO-05	ATCCACAAGCTA

CITE-seq pre-processing and filtering.

Sequencing reads from HTO and ADT libraries were counted using the Kallisto-KITE workflow [<https://github.com/pachterlab/kite>]. Sequencing reads from GEX and TCR $\alpha\beta$ libraries were aligned and

assembled using the Cell Ranger (v7.0.0) software yielding 19.414 and 26.739 reads per cell from the GEX libraries from the two reactions, respectively. Initially filtering removed cell barcodes having less than 300 genes detected or more than 40% of unique molecular identifiers (UMIs) derived from mitochondrial transcripts. Further filtering was done following “overclustering” with `scrn::clusterCells` clustering (NNGraphParam with $k=5$) and removal of clusters having low UMI counts, low number of genes detected and high fraction of UMIs derived from mitochondrial transcripts. Hashtagged cells were demultiplexed into their respective conditions and cross-sample doublets removed using the `hashsolo` function from the `solo` python library³. Intra-sample doublets were removed using `scDblFinder` R package⁴. Expression values the two separate segmentation reactions were sequencing-depth corrected using `batchelor::multiBatchNorm` in R before being integrated for visualization and clustering based on both gene- and surface protein expression using `TotalVI`⁵ with recommended parameters and using the top 1000 variable genes (using the separate reactions as `batch_key`) and including cell cycle “S” and “G2M” scores from `Seurat::CellCycleScoring` as continuous covariates when training to model (to reduce clustering based on cell cycle status). Cell types were annotated based on their expression of distinct lineage surface markers (from the ADT modality; see supplementary figure 2). Malignant T cells were identified based on their monoclonal T-cell receptor (TCR)- β CDR3 region (from `TCR $\alpha\beta$` modality) and high expression of malignant-associated genes such as `TOX` and `KIR3DL2`. Matched skin and blood samples from six Sézary syndrome patients from a previous study by Herrera et al⁶. (GEO accession GSE171811) were preprocessed similar to the CITE-seq samples generated in this study.

CITE-seq differential gene expression, gene-set enrichment, and transcription factor activity analysis and HDACi resistance gene-set scoring.

Following removal of genes that were expressed by less than 10 cells in the dataset resulted in 11,444 genes for downstream analysis. Differentially expressed genes (DEG) were identified based on pairwise T-test comparisons of Malignant T cells between treated (SE, Romidepsin and Romidepsin + SE) and untreated (PBS) conditions with an FDR threshold of 0.05 and only including genes with a \log_2 fold change above 0.5. This yielded 453, 132 and 417 DEG from the SE, Romidepsin and Romidepsin + SE comparisons, respectively. Gene-set enrichment analysis (GSEA) was conducted against the Reactome database using the `ReactomePA::gsePathway` R function with a p-value cutoff of 0.05. Transcription factor (TF) activity was analyzed using the `decoupleR` R package⁷ following the recommended guidelines. In short, TF signatures were extracted from the DoRothEA database with confidence levels A, B or C. Correlated TF signatures above 0.9 were merged into one signature using `decoupleR::check_corr`. TF activity scores were calculated using `decoupleR::run_wmean` with recommended parameters. Differentially activated TF were identified based on pairwise T-test comparisons of TF activity scores from Malignant T cells between treated (SE, Romidepsin and Romidepsin + SE) and untreated (PBS) blood conditions as well as between matched untreated blood and skin with an FDR threshold of 0.05 and only including TF activities with a \log_2 fold change above 0.5. All plots from CITE-seq experiments were constructed using the `ggplot2` R package. HDACi resistance gene-sets

were downloaded from Andrews et al. 2019⁸ including known resistance pathways (ABC Transporters, MAPK/PI3K, NFKB and JAK/STAT genes) as well as differentially up- and down-regulated genes (log2 fold change > 2 and adjusted p-value < 0.05) between HDACi-resistant and sensitive CTCL patients (see table below). These gene-sets were scored in the CITE-seq data using the UCell R package⁹.

HDACi resistance gene-sets:

Gene-set	Genes
ABC Transporters	ABCA1, ABCA10, ABCA11P, ABCA12, ABCA13, ABCA17P, ABCA2, ABCA3, ABCA4, ABCA5, ABCA6, ABCA7, ABCA8, ABCA9, ABCB1, ABCB10, ABCB4, ABCB5, ABCB6, ABCB7, ABCB8, ABCB9, ABCC1, ABCC10, ABCC11, ABCC12, ABCC13, ABCC2, ABCC3, ABCC4, ABCC5, ABCC5-AS1, ABCC6, ABCC6P1, ABCC8, ABCC9, ABCD1, ABCD2, ABCD3, ABCD4, ABCE1, ABCF1, ABCF2, ABCF3, ABCG1, ABCG2, ABCG4, ABCG5
MAPK/PI3K	MAPK1, MAPK10, MAPK11, MAPK12, MAPK13, MAPK14, MAPK1IP1L, MAPK3, MAPK4, MAPK6, MAPK7, MAPK8, MAPK8IP1, MAPK8IP3, MAPK9, MAPKAP1, MAPKAP2, MAPKAP3, MAPKAP5, MAPKAP5-AS1, MAPKBP1, MAP2K1, MAP2K2, MAP2K3, MAP2K4, MAP2K4P1, MAP2K5, MAP2K6, MAP2K7, PIK3C2A, PIK3C2B, PIK3C2G, PIK3C3, PIK3CA, PIK3CB, PIK3CD, PIK3CG
NFKB	NFKB1, NFKB2, NFKBIA, NFKBIB, NFKBID, NFKBIE, NFKBIL1, NFKBIZ, RELA, RELB, IKBIP, IKBKAP, IKBKB, IKBKE, IKBKG
JAK/STAT	STAT1, STAT2, STAT3, STAT4, STAT5A, STAT5B, STAT6, JAK1, JAK2, JAK3
Romidepsin resistant CTCL (Andrews et al. 2019)	CD7, AP1M2, TCL1A, HLA-G, IFI27, S100B, PARD3B, LAIR2, PHGDH, RAB25, RASGRF2, CKAP2L, EPCAM, BAG2, IGHG1, NRP2, STAP1, PLXNA4, HMMR, CDCA7L, IGFL2, AUTS2, MEST, AR, CDC45, GINS2, PRKCQ-AS1, CDC20, C6orf201, CCNB2, IGKV3-11, CDK1, SUS4, TYMS, TRDC, PERP, CCR6, VCAM1, MZB1, ARHGAP32, C1QC, MYBL2, DEFA1, ANXA3, GSTM1, MS4A3, CTSG, DEFA4, CXCL10, GOLGA8G, ITGA11, TCN1
Romidepsin sensitive CTCL (Andrews et al. 2019)	CD160, IFNG, LINC00885, UNC5CL, PPM1H, CCL5, CYB561, RHOU, KCNMA1, ZNF683

Supplementary References

1. Verbrugh HA, Peters R, Rozenberg-Arska M, Peterson PK, Verhoef J. Antibodies to cell wall peptidoglycan of *Staphylococcus aureus* in patients with serious staphylococcal infections. *J Infect Dis.* 1981;144(1):1-9.
2. Mimitou EP, Cheng A, Montalbano A, et al. Multiplexed detection of proteins, transcriptomes, clonotypes and CRISPR perturbations in single cells. *Nature Methods.* 2019;16(5):409-412.
3. Bernstein NJ, Fong NL, Lam I, Roy MA, Hendrickson DG, Kelley DR. Solo: Doublet Identification in Single-Cell RNA-Seq via Semi-Supervised Deep Learning. *Cell Syst.* 2020;11(1):95-101 e105.
4. Germain PL, Lun A, Garcia Meixide C, Macnair W, Robinson MD. Doublet identification in single-cell sequencing data using scDblFinder. *F1000Res.* 2021;10:979.
5. Gayoso A, Steier Z, Lopez R, et al. Joint probabilistic modeling of single-cell multi-omic data with totalVI. *Nat Methods.* 2021;18(3):272-282.

6. Herrera A, Cheng A, Mimitou EP, et al. Multimodal single-cell analysis of cutaneous T-cell lymphoma reveals distinct subclonal tissue-dependent signatures. *Blood*. 2021;138(16):1456-1464.
7. Badia IMP, Velez Santiago J, Braunger J, et al. decoupleR: ensemble of computational methods to infer biological activities from omics data. *Bioinform Adv*. 2022;2(1):vbac016.
8. Andrews JM, Schmidt JA, Carson KR, Musiek AC, Mehta-Shah N, Payton JE. Novel cell adhesion/migration pathways are predictive markers of HDAC inhibitor resistance in cutaneous T cell lymphoma. *EBioMedicine*. 2019;46:170-183.
9. Andreatta M, Carmona SJ. UCell: Robust and scalable single-cell gene signature scoring. *Comput Struct Biotechnol J*. 2021;19:3796-3798.